Available online at www.sciencedirect.com

ScienceDirect

Dyes and Pigments 76 (2008) 624–631

DYES and PIGMENTS

www.elsevier.com/locate/dyepig

Nickel(II) and copper(II) complexes containing 2-(2-(5-substitued isoxazol-3-yl)hydrazono)-5,5-dimethylcyclohexane-1,3-dione ligands: Synthesis, spectral and thermal characterizations

Zhimin Chen [a,b,*], Yiqun Wu [a,b], Donghong Gu [a], Fuxi Gan [a]

[a] *Shanghai Institute of Optics and Fine Mechanics, Chinese Academy of Sciences, Shanghai 201800, PR China*
[b] *Laboratory of Functional Materials, School of Chemistry and Materials Science, Heilongjiang University, Harbin 150080, PR China*

Received 27 August 2006; received in revised form 23 November 2006; accepted 30 November 2006
Available online 17 January 2007

Abstract

Two new hydrazone chelating ligands, 2-(2-(5-methylisoxazol-3-yl)hydrazono)-5,5-dimethylcyclohexane-1,3-dione (HL^1) and 2-(2-(5-*tert*-butylisoxazol-3-yl)hydrazono)-5,5-dimethylcyclohexane-1,3-dione (HL^2), and their nickel(II) and copper(II) complexes were synthesized using the procedure of diazotization, coupling and metallization. Their structures were postulated based on elemental analysis, ^{1}H NMR, ESI-MS, FT-IR spectra and UV–vis electronic absorption spectra. Smooth films of these complexes on K9 glass substrates were prepared using spin-coating and their absorption properties were evaluated. The thermal properties of the metal(II) complexes were investigated by thermogravimetry (TG) and differential thermogravimetry (DTG). Different thermodynamic and kinetic parameters namely activation energy (E^*), enthalpy of activation (ΔH^*), entropy of activation (ΔS^*) and the free energy change of activation (ΔG^*) were calculated using the Coats–Redfern (CR) equation.

Keywords: Hydrazones; Metal(II) complexes; Spin-coating film; Absorption spectra; Thermal property

1. Introduction

As the need for ever-increasing storage capacities continues to grow, new optical storage disc formats have been developed and are now ready for mass commercialization: blu-ray discs (BDs) and high-density DVDs (HD-DVDs) use blue-laser diodes ($\lambda = 405$ nm) with a shorter wavelength that can write smaller bits and thus increase the data storage capacity to 15–100 Gbytes, enough to provide compatibility with high-definition television (HDTV) [1–3]. For write-once discs, the choice of the recording material is between a spin-coated dye, a phase-change layer, and an inorganic alloy. In such discs, a simple and cost-effective organic dye layer can possibly replace the more complex phase-change or inorganic alloy recording stack. For this purpose, a dye material has to be developed that responds sensitively to the wavelength of a blue-violet laser. Moreover, it has to be highly soluble in organic solvent for easy production by a spin-coating process, during which it should perfectly fill narrow grooves, and it should decompose under blue-laser irradiation without melting. Consequently, intensive efforts are now being increasingly made to seek for new organic storage materials with short wavelength absorption and new preparation approaches to obtain high quality recording films in recent years [4–8]. As a very important kind of functional materials, hydrazones and their corresponding metal complexes have attracted much attention over the past years in synthetic chemistry and inorganic chemistry due to their diverse biological activities and various chelating forms [9,10]. Recently, we have reported that some mononuclear metal(II) complexes with

---

* Corresponding author. Shanghai Institute of Optics and Fine Mechanics, Chinese Academy of Sciences, No. 390, Qinghe Road, Jiading District, P.O. Box 800-211, Shanghai 201800, PR China. Tel.: +86 21 69918592; fax: +86 21 69918800.

E-mail address: zmchen@siom.ac.cn (Z. Chen).

0143-7208/$ - see front matter
doi:10.1016/j.dyepig.2006.11.009

absorption bands in the blue-violet light region, matching the 405 nm short wavelength laser, are suitable for application in high-density recordable optical storage [11–13]. In this paper, we report on the syntheses of four nickel(II) and copper(II) complexes containing 2-(2-(5-substitued isoxazol-3-yl)hydrazono)-5,5-dimethylcyclohexane-1,3-dione ligands. Their chemical structures are shown in Fig. 1. The relationships of the absorption bands from metal(II) complexes with different metal(II) ions to ligands and the structures of the metal(II) complexes were discussed. It can be expected that the relationships will guide the syntheses of new materials for the later application. Furthermore, we also studied the thermal properties of these metal(II) complexes and the solubility in organic solvents as well as the absorption behaviors of their films. In addition, different thermodynamic and kinetic parameters namely activation energy (E^*), enthalpy of activation (ΔH^*), entropy of activation (ΔS^*) and free energy change of activation (ΔG^*) are calculated using Coats–Redfern (CR) equation. All these preliminary properties indicate that these metal(II) complexes have a promising use in high-density digital versatile disc-recordable systems for next generation optical storage.

2. Experimental

2.1. Materials

All chemicals and solvents in this work were of analytical grade and were used as-received. 3-Amino-5-methylisoxazole and 5,5-dimethylcyclohexane-1,3-dione used in the synthesis of the hydrazone dyes were purchased from Acros Chemical Co. and were used without further purification. 3-Amino-5-*tert*-butylisoxazole was prepared according to the literature [14]. The product was filtrated with a great deal of water and dried as yellowish needles (mp. 120–121 °C). A facile route was adopted in the synthesis of the ligands (HL^1 and HL^2) and their nickel(II) and copper(II) complexes and the synthetic schemes together with suggested structures are shown in Fig. 1.

2.2. Instrument and methods

The melting points of the compounds were determined using an X-4 microscopic melting point apparatus (made in China) and were uncorrected. Elemental analyses of C, H and N were carried out on a Vario EL elemental analyzer. Metal(II) contents were estimated by complexometric EDTA titration (after complete decomposition of the complexes in concentrated nitric acid several times) using murexide as indicator in buffer (NH_3–NH_4Cl solution) and calculated from the expression $X\% = C_{EDTA} \times V_{EDTA} \times M/m_s$, where X is the metal content of sample, C_{EDTA} is the concentration of EDTA titrant, V_{EDTA} is the volume of EDTA used in titration, m_s is the mass of sample and M is the molecular weight. FT-IR spectra were obtained in KBr pellets on a Nicolet Avatar 360 FT-IR spectrometer in the 4000–400 cm^{-1} region. ^1H NMR spectra ($CDCl_3$ solutions) were recorded at 500 MHz on a Bruker Avance AV-500 instrument with tetramethylsilane (TMS) as an internal standard. EI and ESI mass spectra were performed using an Agilent spectrometer (HP 5973N, at 70 eV) and a Mariner LC-TOF spectrometer using electrospray ionization, respectively. UV–vis spectra were measured using a Perkin–Elmer Lambda 9 UV/VIS/NIR spectrophotometer. Thermal properties were analyzed with a Perkin–Elmer Instruction system (TGA-7) at a heating rate of 10 °C min^{-1} under a nitrogen atmosphere.

2.3. Synthesis of 2-(2-(5-methylisoxazol-3-yl)hydrazono)-5,5-dimethylcyclohexane-1,3-dione ligand (HL^1)

2.3.1. Diazotization

3-Amino-5-methylisoxazole (2.000 g, 0.020 mol) was dissolved in 40 ml concentrated phosphoric acid (85%) at room temperature. The solution was then cooled to −5 to 0 °C in an ice-salt bath and maintained at this temperature while a solution of sodium nitrite (1.520 g, 0.022 mol) in water (10 ml) was added dropwise within 1 h with continuous stirring; the ensuing mixture was stirred at 0–5 °C for a further

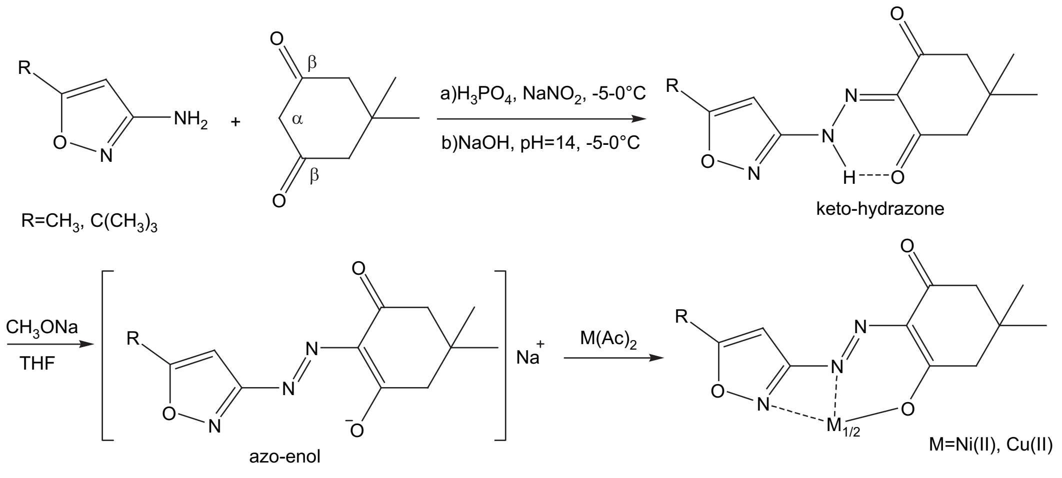

Fig. 1. Synthetic schemes of ligands (HL^1 and HL^2) and their nickel(II) and copper(II) complexes.

1 h. The resulting diazonium solution was used directly in the coupling step.

2.3.2. Coupling

The coupling component (5,5-dimethylcyclohexane-1,3-dione, 3.080 g, 0.022 mol) was dissolved in 200 ml sodium hydroxide solution (2%, pH = 14) and cooled to −5 to 0 °C in an ice-salt bath. The above diazonium solution was added to the stirred coupling component solution at −5 to 0 °C over 30 min, maintaining the pH at 8–10. The mixture was allowed to rise to room temperature over 4 h and the pH was lowered to about 5. The precipitated solid was collected by filtration, washed with water, and then vacuum dried. The crude product was finally recrystallized from ethyl acetate to form yellow crystals. Yield: 4.050 g (81%). mp. 182–183 °C. Anal. Calcd (found) for $C_{12}H_{15}N_3O_3$: C, 57.82 (57.76); H, 6.07 (6.04); N, 16.86 (16.67). ^1H NMR ($CDCl_3$, TMS, δ ppm): 1.134 (s, 6H, $>C(CH_3)_2$), 2.440 (s, 3H, $-CH_3$), 2.634–2.642 (d, $J = 4.0$, 4H, CH_2), 6.493 (s, 1H, isoxazole-H), 14.848 (s, br, 1H, hydrazone NH). Electronic absorption spectrum (UV–vis) in chloroform: λ_{max} (nm) ($\log \varepsilon$) = 347 (4.29). FT-IR spectra ν: 3441, 3064, 2956, 2935, 2889, 1680, 1651, 1612, 1524, 1462, 1361, 1265, 1190, 1116, 977, 919, 802, 561 cm^{-1}. EI-MS found (Calcd): $m/z = 249$ (249) [M^+].

2.4. Synthesis of 2-(2-(5-tert-butylisoxazol-3-yl)hydrazono)-5,5-dimethylcyclohexane-1,3-dione ligand (HL^2)

The ligand (HL^2) was synthesized by a procedure similar to that of the ligand (HL^1) except that 3-amino-5-*tert*-butylisoxazole (2.800 g, 0.020 mol) was used. Yield: 5.200 g (89%). mp. 121–122 °C. Anal. Calcd (found) for $C_{15}H_{21}N_3O_3$: C, 61.84 (61.79); H, 7.27 (7.14); N, 14.42 (14.37). ^1H NMR ($CDCl_3$, TMS, δ ppm): 1.136 (s, 6H, $>C(CH_3)_2$), 1.357 (s, 9H, $-C(CH_3)_3$), 2.641–2.647 (d, $J = 3.0$, 4H, CH_2), 6.454 (s, 1H, isoxazole-H), 14.885 (s, br, 1H, hydrazone NH). Electronic absorption spectrum (UV–vis) in chloroform: λ_{max} (nm) ($\log \varepsilon$) = 349 (4.30). FT-IR spectra ν: 3440, 3111, 2964, 2931, 2870, 1697, 1649, 1599, 1516, 1460, 1360, 1277, 1184, 1115, 976, 926, 785, 561 cm^{-1}. EI-MS found (Calcd): $m/z = 291$ (291) [M^+].

2.5. General procedure for the synthesis of the metal(II) complexes

The metal(II) complexes were prepared by the same general method: the resulting ligand (2.0 mmol) was dissolved in 30 ml absolute tetrahydrofuran (THF) and 2 ml sodium methoxide (1 mol/l) solution at room temperature and the metal(II) acetate (1.0 mmol) dissolved in 10 ml tetrahydrofuran was added dropwise under vigorous stirring. The ensuing mixture was stirred at room temperature overnight and 10 ml water was added. The precipitated solid was collected by filtration, washed with water and then vacuum dried to obtain the metal(II) complex. The crude product was finally recrystallized from methanol to form brown crystals. Specific details for each compound are given below.

2.5.1. $Ni(L^1)_2$ complex

Yield: 68%. mp. > 275 °C (dec.). Anal. Calcd (found) for $C_{24}H_{28}N_6O_6Ni$: C, 51.92 (51.85); H, 5.08 (5.02); N, 15.14 (15.08); Ni, 10.57 (10.86). Electronic absorption spectrum (UV–vis) in chloroform: λ_{max} (nm) = 421, 361, 335, 274. FT-IR spectra ν: 3442, 2955, 2928, 2818, 1657, 1608, 1564, 1468, 1321, 1250, 1190, 1047, 819, 584, 503, 461 cm^{-1}. ESI-MS Calcd (found): $m/z = 554.1$ (555.5) [$M + H^+$].

2.5.2. $Ni(L^2)_2$ complex

Yield: 64%. mp. > 270 °C (dec.). Anal. Calcd (found) for $C_{30}H_{40}N_6O_6Ni$: C, 56.36 (56.02); H, 6.31 (6.51); N, 13.14 (13.21); Ni, 9.18 (9.02). Electronic absorption spectrum (UV–vis) in chloroform: λ_{max} (nm) = 422, 359, 336, 276. FT-IR spectra ν: 3442, 2962, 2926, 2819, 1672, 1592, 1564, 1464, 1319, 1269, 1184, 1041, 817, 588, 509, 459 cm^{-1}. ESI-MS Calcd (found): $m/z = 638.2$ (639.5) [$M + H^+$].

2.5.3. $Cu(L^1)_2$ complex

Yield: 77%. mp. > 200 °C (dec.). Anal. Calcd (found) for $C_{24}H_{28}N_6O_6Cu$: C, 51.47 (51.31); H, 5.04 (5.01); N, 15.01 (14.87); Cu, 11.35 (11.18). Electronic absorption spectrum (UV–vis) in chloroform: λ_{max} (nm) = 376, 268. FT-IR spectra ν: 3437, 2955, 2929, 2870, 1664, 1610, 1524, 1324, 1255, 1140, 1007, 927, 503, 469 cm^{-1}. ESI-MS Calcd (found): $m/z = 559.1$ (560.2) [$M + H^+$].

2.5.4. $Cu(L^2)_2$ complex

Yield: 73%. mp. > 180 °C (dec.). Anal. Calcd (found) for $C_{30}H_{40}N_6O_6Cu$: C, 55.93 (55.74); H, 6.26 (6.11); N, 13.05 (13.02); Ni, 9.86 (9.72). Electronic absorption spectrum (UV–vis) in chloroform: λ_{max} (nm) = 377, 269. FT-IR spectra ν: 3441, 2968, 2933, 2873, 1674, 1593, 1533, 1344, 1273, 1196, 1061, 941, 505, 467 cm^{-1}. ESI-MS Calcd (found): $m/z = 643.2$ (644.4) [$M + H^+$].

2.6. Preparation of the spin-coated thin films

The solutions were prepared by dissolving the respective metal(II) complex in 2,2,3,3-tetrafluoro-1-propanol (TFP) and $CHCl_3$ (10:1) to give a concentration of 30 mg ml^{-1}. The solution was filtered through a 0.22 μm millipore membrane filter to obtain the coating solution. The K9 glass substrates (diameter 30 mm) were cleaned in an ultrasonic bath with acetone, ethanol and deionized water for several times and dried, successively. The films were prepared with a KW-4A precision spin-coater (Chemat Technology Inc.) using a syringe. A two-step procedure, 800 rpm for the first 4 s and 3000 rpm thereafter for 40 s, was used to prepare smooth films. The substrates were kept at room temperature and 50% relative humidity throughout the deposition process. The resulting films were heated at 50 °C for 2–3 h to ensure removal of the solvent.

3. Results and discussion

3.1. Synthesis and characterization

Classic keto-hydrazone pigments are prepared by aqueous diazotization and coupling, which lead directly to a pure product in high yield and in a physical form suitable for application [15]. It has been reported that diazotized heterocyclic amines couple successfully with a range of reactive methylene coupling components in organic solvent in the presence of sodium acetate [16,17]. However, attempts to prepare compounds using this standard method either failed completely or gave a low yield of a highly impure product, probably due to the instability of the isoxazole heterocyclic diazonium salts in hydrochloric acid solution at pH sufficiently high to allow coupling to take place. In the present study, it was found that reasonable yields of the hydrazone pigment containing isoxazoles and 1,3-dicarbonyl compounds ($XC(O)-CH_2-C(O)X$) could be obtained when diazotization was carried out in concentrated phosphoric acid and coupling was undertaken in sodium hydroxide solution.

The dyes prepared in this study may exist in the hydrazo-keto and azo-enol tautomeric forms as shown in Fig. 1. It has been shown, conclusively from a series of investigations using various techniques, such as IR, NMR, and X-ray crystallography, that hydrazones containing 1,3-dicarbonyl groups exist exclusively in the keto-hydrazone form both in solution and in the solid state [18–20]. An intramolecular hydrogen bridge linking one of the carbonyl groups to the NH-moiety of the hydrazone unit was found to be a characteristic feature of this compound class. The six-membered, intramolecular hydrogen bonding ring is possible in the keto-hydrazone tautomer as shown in Fig. 1. The infrared spectra of hydrazones based on a substituted 1,3-dione and, in particular the position of the carbonyl stretching vibrations, have been of considerable importance in establishing that the compounds exist exclusively in the keto-hydrazone form. The solid state IR spectra of the synthesized hydrazones show two intense carbonyl absorption bands (HL^1: 1680 ($\nu C{=}O$), 1651 ($\nu C{=}O \cdots H$); HL^2: 1697 ($\nu C{=}O$), 1649 ($\nu C{=}O \cdots H$) cm^{-1}) consistent with a keto-hydrazone form with extensive six-membered intramolecular hydrogen bonding, and this has been confirmed by a number of previous published reports of keto-hydrazone analogues [18,20]. Another typical feature of the free ligands is the existence of an NH vibration around 3100 cm^{-1} which affords proof of the H-bonded hydrazone structure in the solid state also; the remaining vibrational frequencies obtained and their tentative assignments are shown in Table 1. In the ^1H NMR spectra of the ligands, the hydrazone protons appear as a broad singlet at 14.848 ppm for HL^1 and 14.885 ppm for HL^2, which is a clear indication of a protonated nitrogen atom adjacent to the isoxazole unit. Moreover, the two methylene groups of the cyclohexane-1,3-dione moiety yield separate singlet-signals at around 2.64 ppm in the proton spectra. Non-equivalency of the two methylene groups also gives a manifestation of the six-membered H-bonded ring involving one of the carbonyl groups and the protonated nitrogen of the hydrazone structure. The obtained IR spectra, ^1H NMR, EI mass spectra and elemental analytical data agree well with the formulae of the ligands.

The nickel(II) and copper(II) complexes, $M(L)_2$ [M = Ni (II), Cu(II)], were synthesized by reaction of the relevant metal(II) acetate with the hydrazone ligands. Syntheses of the four metal(II) complexes were essentially the same and involved heating and stirring of stoichiometric amounts of the hydrazone ligand and the metal(II) acetate in tetrahydrofuran. The direct use of sodium methoxide solution is characteristic of the present synthetic method. Due to the possible hydrazo-keto and azo-enol tautomerism of the prepared hydrazones [21], the action of sodium alkoxide on the hydrazone ligands in solution is to convert the hydrazo-keto form into the azo-enol form [11,22]. Consequently, metal(II) complexes were easily synthesized by chelation of the metal(II) ion and ligand in the azo-enol form (see Fig. 1). The desired complexes were readily crystallized from the reaction solution by the addition of a small amount of water. Removal of solvent under vacuum gave the corresponding products, in good yield, which were stable in solution as well as in the dry state under ambient conditions. These metal(II) complexes not only could be easily dissolved in aprotic solvents such as DMF and DMSO, but also could be dissolved in many weakly polar organic solvents such as toluene, chloroform, ethyl acetate and tetrahydrofuran. This solubility may be due to the substituted *tert*-butyl and methyl groups which increase repulsion between and thereby reduce the aggregation of molecules. Their solubility decreases in strongly polar solvents such as methanol, ethanol and water, because the alkyl groups and other substituted groups are lipophilic and weakly polar. In addition, it is found that the *tert*-butyl-substituted hydrazone (HL^2) and its metal(II) complexes show better solubility than the methyl-substituted hydrazone (HL^1) and its metal(II) complexes in the same solvent, but the solubility of the complexes with the

Table 1
Significant FT-IR bands and tentative assignments of the ligands and their metal(II) complexes

Compound	νH–N (hydrazone)	$\nu_s CH(CH_3)$	$\nu C{=}O$	$\nu C{=}O \cdots H$	$\nu CH{=}N$ (isoxazole)	$\nu N{-}N{=}C$ (azomethine)	$\nu N{=}N$	$\nu C{-}O$ (enol hydroxyl)	M–N	M–O
HL^1	3064	2956, 2935, 2889	1680	1651	1612	1462	–	–	–	–
HL^2	3111	2964, 2931, 2870	1697	1649	1599	1460	–	–	–	–
$Ni(L^1)_2$	–	2955, 2928, 2818	1657	–	1608	–	1321	1250	461	503
$Cu(L^1)_2$	–	2955, 2929, 2870	1664	–	1610	–	1324	1255	469	503
$Ni(L^2)_2$	–	2962, 2926, 2819	1672	–	1592	–	1319	1269	459	509
$Cu(L^2)_2$	–	2968, 2933, 2873	1674	–	1593	–	1344	1273	467	505

same ligand is little different. The elemental analytical data, ESI mass spectra and FT-IR spectra of the metal(II) complexes agree well with their formulae. The metal-to-ligand ratios of the copper(II) and nickel(II) complexes were found to be 1:2 and, thus, the metal(II) ions appear to be hexa-coordinated with the *O*,*N*,*N′*-monobasic tridentate ligands and the probable geometry is octahedral for metal(II) ions [23,24]. Fig. 1 shows the suggested structures of the metal(II) complexes.

3.2. FT-IR spectra of the ligands and their metal(II) complexes

The important IR characteristic absorption bands of the ligands and their four metal(II) complexes, along with their proposed assignments, are summarized in Table 1. As seen from Table 1, the IR spectra of the four metal(II) complexes were similar to each other, except for some slight shifts and intensity changes of a few vibration bands caused by different substituted groups and metal(II) ions, which indicate that the complexes were of similar structure. However, there were some significant differences between the metal(II) complexes and their free ligands upon chelation, as expected. The coordination mode and sites of the ligands to the metal(II) ions were investigated by comparing the infrared spectra of the free ligands with their metal(II) complexes. Upon coordination, it is noteworthy that the peak at 1657–1674 $\mathrm{cm^{-1}}$ attributed to νC=O vibration, was shifted by 20–30 $\mathrm{cm^{-1}}$ on complexation, while the second carbonyl absorption band at ~1650 $\mathrm{cm^{-1}}$, appearing in the spectra of the free ligands with the extensive six-membered intramolecular hydrogen bonded structure, was not observed. These results indicate that the ligands are in the azo-enol form in the complex which naturally forms an enolic hydroxyl oxygen and an enol carbonyl with consequent replacement of the enolic hydrogen by the metal(II) ion [25,26]. A new band due to the νC–O appearing at 1250–1273 $\mathrm{cm^{-1}}$ in the spectra of all complexes can be further evidence for the bonding of the enol hydroxyl oxygen to the metal(II) ion. Furthermore, the medium-intensity band at 3064–3111 $\mathrm{cm^{-1}}$ of the free ligands, due to νNH stretching, disappears in the complexes, suggesting that the NH proton is lost via enolization and the resulting enolic oxygen and azoic nitrogen take part in coordination [27,28]. Moreover, the ν–N–N=C– absorption band at 1460–1462 $\mathrm{cm^{-1}}$, appearing in the spectra of free ligands, is not observed but a new band due to –N=N– vibration appears around 1319–1344 $\mathrm{cm^{-1}}$ in the spectra of all complexes, which supports the azo-enol form of the ligands in the metal(II) complexes; the appearance of this peak at relatively lower field may indicate coordination via the N=N group [29–31]. In addition, the IR spectrum of the ligands reveals a sharp band at ~1600 $\mathrm{cm^{-1}}$ corresponding to the νC=N of the isoxazole ring, which is shifted to a lower frequency by about 2–6 $\mathrm{cm^{-1}}$ after complexation in all complexes, suggesting that the nitrogen atom of the isoxazole ring also contributes to complexation [32–34]. The mode of bonding of the metal(II) ion is further supported by the broad absorption bands in the region 503–509 and 459–469 $\mathrm{cm^{-1}}$, which can be assigned to νM–O and νM–N stretching vibrations, respectively [32,33]. Therefore, from these IR spectra, it is concluded that the ligands may exist in the azo-enol form during complexation and behave as a *O*,*N*,*N′*-monobasic tridentate ligand coordinated to the metal(II) ions via the deprotonated enolic *O*, azoic group *N* and isoxazole *N*. There are additional factors which might affect the structures of these complexes such as the possibility of various isomeric structures, the bulkiness of the ligands, the nature of the metal(II) ions and intermolecular hydrogen bonds. However, due to instrument limitation, we are not able to explore these further.

3.3. UV–vis electronic absorption spectra of the ligands and their metal(II) complexes

The formation of the metal(II) complexes was also confirmed by UV–vis spectra. The spectra of the free ligands and their metal(II) complexes in $\mathrm{CHCl_3}$ solutions are shown in Fig. 2. The spectra of the uncomplexed ligands give rise to high-energy absorption below 250 nm that is probably due to $\pi \rightarrow \pi^*$ transition of the isoxazole ring moiety. This band is bathochromic shifted by ~30 nm in the spectra of the complexes containing deprotonated ligands, which can be attributed to the overlap of the central-metal-d-orbital with the π-orbital of the donor isoxazole ring, which causes an increase in conjugation in the ligand molecule and thus lowers the $\pi \rightarrow \pi^*$ transition. The strong absorption band in the 347–349 nm range of the free ligands is assignable to the $n \rightarrow \pi^*$ transition originating from the azomethine linkage of the hydrazone (–NH–N=C–) moiety [35,36]. Both the position and intensity of this band show dependence on the nature of the substituents within the isoxazole moiety of the ligands. The presence of the electron donating group (–C($\mathrm{CH_3}$)$_3$) in $\mathrm{HL^2}$ shifts the $n \rightarrow \pi^*$ transition to lower energy compared to the –$\mathrm{CH_3}$ group in $\mathrm{HL^1}$. This red shift can be attributed to increased conjugation. In the spectra of the metal(II) complexes, the bands on the high wavelength side

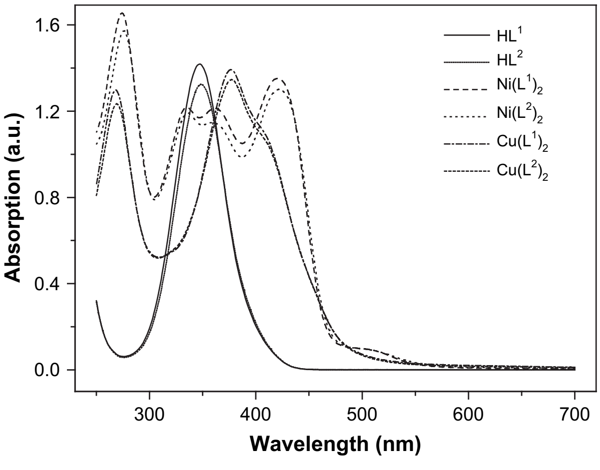

Fig. 2. Absorption spectra of the ligands and their metal(II) complexes in chloroform.

show that there is significant change in the energy of the n → π* band on complexation. For the two Ni(II) complexes, successive splitting of the n → π* bands appeared at 421, 361, and 335 nm for $Ni(L^1)_2$ and 422, 359, and 336 nm for $Ni(L^2)_2$, respectively, while the two Cu(II) complexes display a broad envelop with a shoulder of low extinction at 376–377 nm. The significant changes in the spectrum of the metal(II) complexes most likely originate from metallization enforced by the chelated metal(II) ion which can readily convert the keto-hydrazone form into the azo-enol form, increase conjugation and delocalization of the whole electronic system and result in the observed energy level change of the n → π* transition of the conjugated chromophore [11,13]. The results clearly indicate that the ligands coordinate to metal(II) ions, which is in accordance with the results of the FT-IR spectra. Furthermore, in the case of the Ni(II) complexes, a band in the visible region is observed at 510 nm as a low intensity shoulder. This band is considered to arise from the forbidden d–d transition, which is generally too weak. The expected d–d transition in the visible region for the Cu(II) complexes could not be detected, perhaps because it was lost in the low-energy tail of the intense charge transfer transition [27]. In addition, from Fig. 2, it is evident that the ability of the metal(II) ions to impart bathochromic shifts in the absorption maximum λ_{max} on the high wavelength side is Ni(II) > Cu(II). This indicates that the nature of the metal(II) ions affects the position of the absorption band significantly. According to modern molecular orbital theory [37], any factor that can influence the electronic density of a conjugated system must result in the bathochromic or hypsochromic shift of the absorption band. Here, in the case of the metal(II) complexes with the same ligand the main cause of the bathochromic shift is generally related to the electronegativity of the metal(II) ion. The order of the electronegativity of the metal(II) ions is Ni^{2+} (1.91) > Cu^{2+} (1.90) [38]. The larger the electronegativity, the greater the ability of the metal(II) ions to attract the unbonded electrons from the deprotonated enolic *O*, azoic group *N* and isoxazole *N*, and so the n electronic density in the conjugated system is increased, the energy difference of n → π* transition is reduced and the bathochromic shift of the absorption band is enhanced. Besides the electronegativity of the metal(II) ions, there are other factors, such as distortion, electronic shell structure and the radius of the metal(II) ions, that probably work in combination with and contribute to the absorption band shifts.

We also prepared solid thin films of the metal(II) complexes on K9 substrates by spin-coating and studied the absorption spectra of the thin films. As shown in Fig. 3, the thin films show similar absorption bands compared with those obtained in chloroform solution. However, the obvious broadening and shifts of the absorption bands are also observed. These changes originate from extensive excitation coupling between adjacent conjugated molecules, as observed earlier in other complexes [38]. The metal(II) complex films show typical electronic absorption spectra with blue-violet light absorption at about 330–430 nm, which have sharp tails in the longer wavelength region and an absorbance on the 405 nm side. Therefore, these characteristics indicate that the metal(II) complexes have potential application for high-density optical recording media which can be recorded and read at a short wavelength laser (blue laser) of 405 nm [11,13].

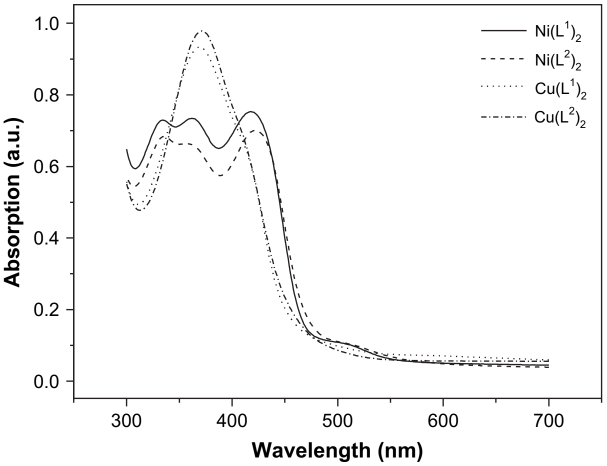

Fig. 3. Absorption spectra of the metal(II) complex films on K9 glass substrates.

3.4. Thermal properties of the metal(II) complexes

The thermal properties of the metal(II) complexes were investigated by thermogravimetric analysis (TGA) and differential thermogravimetry (DTG). Fig. 4 shows the recorded TGA and DTG curves of the four metal(II) complexes under a nitrogen atmosphere; important data are summarized in Table 2. It can be seen that the TGA curves of the complexes show no mass loss up to 180 °C, indicating the absence of water molecules and any other adsorptive solvent molecules in the coordination sphere. As the temperature is increased, the TGA and DTG curves exhibit a sharp mass loss at about 180–280 °C. For the $Ni(L^1)_2$ and $Ni(L^2)_2$ complexes, the DTG curves are very similar to each other and display sharp mass losses (estimated mass loss 23 and 19%:theoretical 22 and 19%) at 274 and 269 °C, respectively, which are in good agreement with the decomposition of a $C_8H_{12}O$ (5,5-dimethylcyclohex-2-enone) molecule. After the rapid loss of the two complexes, a gradual decomposition over a large temperature range (300–450 °C for $Ni(L^1)_2$ and 300–480 °C for $Ni(L^2)_2$) occurred, which may correspond to degradation of the ligand molecule. In contrast, the $Cu(L^1)_2$ complex displayed single-step decomposition and the process of decomposition was more rapid than that of the former two complexes. This complex was stable up to 195 °C above which drastic mass loss occurred at a rate of about 72% within a narrow temperature range (~10 °C). This process can be readily interpreted as decomposition of two ligand molecules, which is in good agreement with the calculated value (theoretical mass loss, 82%). The $Cu(L^1)_2$ complex completely decomposed to the corresponding metal oxide, CuO, to about 15% of the original mass. For the $Cu(L^2)_2$ complex, sharp mass loss occurred at the lower temperature of

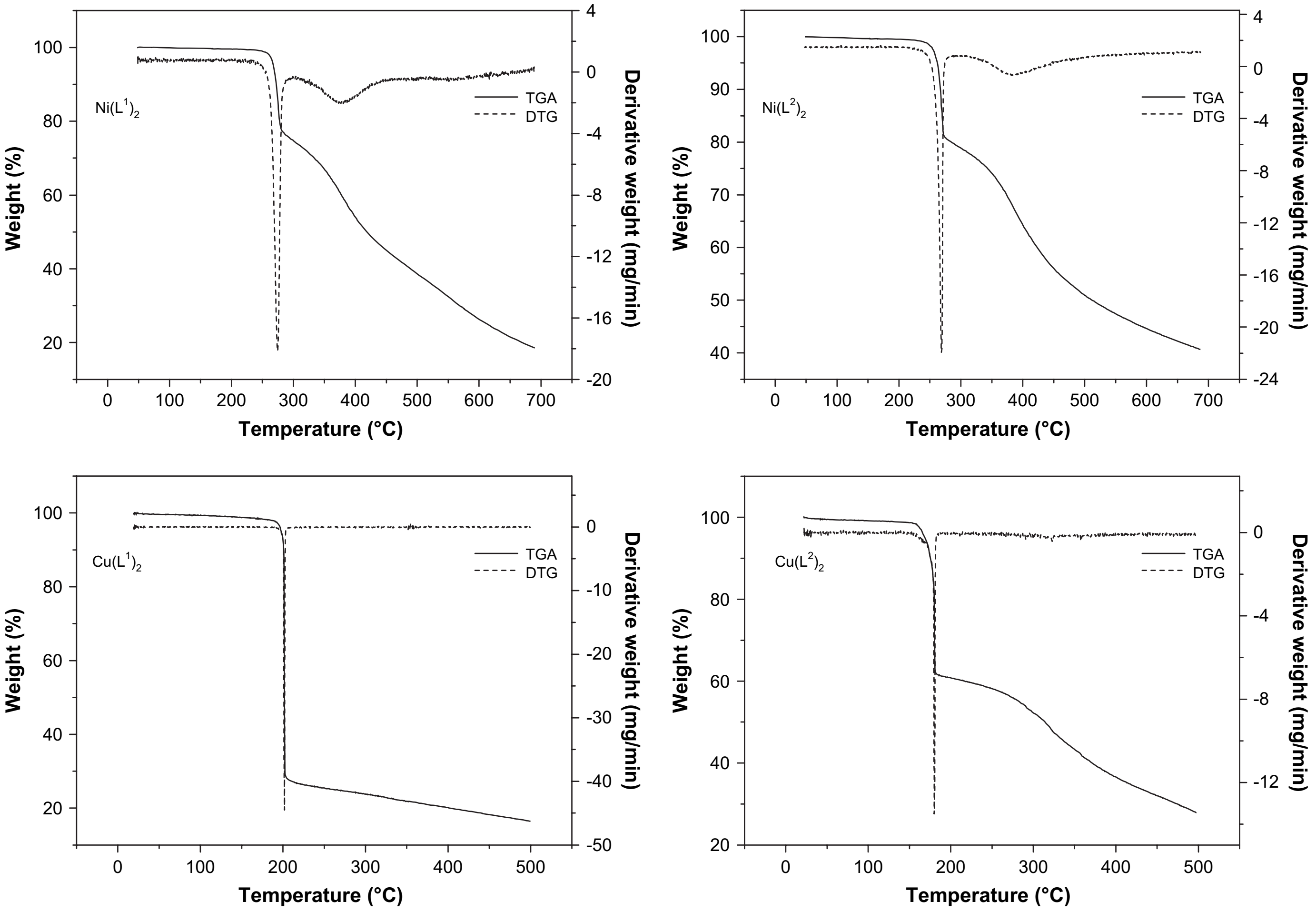

Fig. 4. TGA and DTG curves of the metal(II) complexes.

about 180 °C compared to the other complexes, which may be interpreted as decomposition of one ligand molecule, which is in good agreement with the calculated value (estimated mass loss 38%, theoretical 40%). The degradation of the $Cu(L^2)_2$ complex exhibited a gradual loss in mass over the remaining temperature range and showed no obvious peak in the DTG curve. In addition, from Fig. 4 and Table 2, it is clear that the order of the thermal stability of the metal(II) complexes with the same substituent was Ni(II) > Cu(II) and the *tert*-butyl group in the isoxazole ring resulted in a decrease in stability relative to the corresponding methyl group. The results indicate that the thermal stability of the metal(II) complexes has something to do with their ligands and the nature of the metal(II) ions [39]. These results indicate that the synthesized complexes, especially the Ni(II) complexes, have high thermal stability and a sharp thermal decomposition threshold with high mass loss rate and, therefore, offer the potential to form a small and sharp recording mark edge [25]. With further development, these complexes may ultimately prove to be an important class of high-density, blue-violet light recordable optical disk storage materials.

The kinetic parameters of the decomposition of the complexes namely, activation energy (E^*), enthalpy (ΔH^*), entropy (ΔS^*) and free energy of the decomposition (ΔG^*) as well as the pre-exponential factor (A) were evaluated graphically using the Coats–Redfern [40] relationship:

$$\ln\left[-\ln(1-\alpha)/T^2\right] = -E^*/RT + \ln[AR/\varphi E^*] \qquad (1)$$

Table 2
The thermal behavior and kinetic parameters of the metal(II) complexes

Complex	Temperature range (°C)	%Weight loss found (Calcd)	DTG peak temperature (°C)	E^* (kJ mol^{-1})	A (s^{-1})	ΔS^* (J K^{-1} mol^{-1})	ΔH^* (kJ mol^{-1})	ΔG^* (kJ mol^{-1})
$Ni(L^1)_2$	260–300	23 (22)	274	437.4	1.2×10^{40}	517.3	432.8	149.8
$Ni(L^2)_2$	250–290	19 (19)	269	407.5	4.5×10^{37}	471.0	403.8	147.7
$Cu(L^1)_2$	195–205	72 (82)	202	473.8	6.8×10^{49}	705.3	469.8	134.7
$Cu(L^2)_2$	165–185	38 (42)	180	275.6	8.9×10^{29}	325.0	271.8	124.5

where α is the fraction of sample decomposed at temperature T, A the pre-exponential factor, φ the heating rate, E^* the activation energy, R the gas constant. A plot of $\ln[-\ln(1-\alpha)/T^2]$ against $1/T$ gives a slope from which E^* was calculated and A was determined from the intercept. The entropy of activation (ΔS^*), enthalpy of activation (ΔH^*) and the free energy change of activation (ΔG^*) were calculated using the following equations.

$$\Delta S^* = 2.303R \log(Ah/kT_s) \tag{2}$$

$$\Delta H^* = E^* - RT_s \tag{3}$$

$$\Delta G^* = \Delta H^* - T_s \Delta S^* \tag{4}$$

where k, h and T_s are the Boltzman constant, Planck constant and the DTG peak temperature, respectively.

The calculated values of E^*, A, ΔS^*, ΔH^* and ΔG^* for the decomposition steps are given in Table 2. On comparing the activation energy of the first stage of decomposition for all complexes, the order of the activation energy values of the different metal(II) complexes was $Cu(L^1)_2 > Ni(L^1)_2 > Ni(L^2)_2 > Cu(L^2)_2$, indicating that the rate of decomposition for this stage is of the same order. This difference may be due to the stereostructure of the complexes and the electronic configuration of the metal(II) ion. These results agree well with those of the TG analysis detailed above. The ΔS^* values of the first stage for all complexes were found to be positive, indicating that the activated complex was less ordered than the reactants [41,42].

4. Conclusions

We have described the synthesis and some spectroscopic and thermal properties of two new hydrazones and their four nickel(II) and copper(II) complexes. The possible structures of the ligands and their metal(II) complexes were proposed based on elemental analysis, ^{1}H NMR, ESI-MS, FT-IR spectra and UV–vis electronic absorption spectra. The metal(II) complex films show typical electronic absorption spectra with blue-violet light absorption at about 330–420 nm. They have sharp tails in the longer wavelength region and absorbance at the 405 nm side, which could match the blu-ray laser. The thermal properties of the metal(II) complexes were investigated by thermogravimetry (TG) and differential thermogravimetric analysis (DTG). Different thermodynamic and kinetic parameters (E^*, ΔH^*, ΔS^*, ΔG^*) were calculated using the Coats–Redfern (CR) equation. It was found that the metal(II) complexes offer potential application for high-density disc-recordable system at 405 nm due to their high thermal stability and sharp thermal decomposition threshold with high mass loss rate.

Acknowledgements

We thank the National High Technology Development Program of China (No. 2004AA31G230) and the Science and Technology Development Foundation of Shanghai City (No. 012261068) for providing financial support.

References

[1] Mustroph H, Stollenwerk M, Bressau V. Angew Chem Int Ed 2006;45:2016.
[2] Kuiper AET, van Pieterson L. MRS Bull 2006;31:308.
[3] Nakai T, Tsukamoto T, Ashida S, Yusu K, Yoshida N, Umezawa K, et al. Jpn J Appl Phys 2004;43:4987.
[4] Sabi Y, Tamada S, Iwamura T, Oyamada M, Bruder F, Oser R, et al. Jpn J Appl Phys 2003;42:1056.
[5] Nishiwaki H, Kitano K, Nakajima H, Muramatsu E, Taniguchi S, Inoue A, et al. Jpn J Appl Phys 2006;45:1452.
[6] Kubo H, Shibata M, Katayama K, Takano H, Kakuta T, Usami Y, et al. Proc SPIE 2004;5380:128.
[7] Graciet JC, Eur. Patent nos. 1516894, 1516895, 1517316, 1502917; 2005.
[8] Ishida T, Shiozaki H, Ogiso A, Jpn. Patent nos. 2004330614, 2004306306, 2004306307, 2004291281, 2004291253, 2004249635, 2004243596; 2004.
[9] Carvalho SA, da Silva EF, Santa-Rita RM, de Castro SL, Fraga CAM. Bioorg Med Chem Lett 2004;14:5967.
[10] Rodriguez-Arguelles MC, Ferrari MB, Bisceglie F, Pelizzi C, Pelosi G, Pinelli S, et al. J Inorg Biochem 2004;98:313.
[11] Huang FX, Wu YQ, Gu DH, Gan FX. Mater Lett 2004;58:2461.
[12] Huang FX, Wu YQ, Gu DH, Gan FX. Thin Solid Films 2005;483:251.
[13] Chen ZM, Huang FX, Wu YQ, Gu DH, Gan FX. Inorg Chem Commun 2006;9:21.
[14] Kenneth W, Burow J, Richard F. U.S. Patent no. 4,259,501; 1981.
[15] Christie RM, Standring PN. Dyes Pigments 1988;9:37.
[16] Henecka H, Timmler H, Lorenz R, Geiger W. Chem Ber 1957;90:1060.
[17] Eistert B, Schank K. Chem Ber 1963;96:2304.
[18] Christie RM, Dryburgh WT, Standring PN. Dyes Pigments 1991;16:231.
[19] Christie RM, Hill JM, Rosair G. Dyes Pigments 2006;71:169.
[20] Price CP, Grzesiak AL, Kampf JW, Matzger AJ. Cryst Growth Des 2003;3:1021.
[21] Song HF, Chen KC, Tian H. Dyes Pigments 2002;53:257.
[22] Marchetti F, Pettinari C, Cingolani A, Pettinari R, Rossi M, Caruso F. J Organomet Chem 2002;645:134.
[23] Kessler VG, Gohil S. J Sol-Gel Sci Technol 2000;19:525.
[24] Sabbatini N, Guardigli M, Lehn JM. Coord Chem Rev 1993;123:201.
[25] Huang FX, Wu YQ, Gu DH, Gan FX. Spectrochim Acta Part A 2005;61:2856.
[26] Albert J, Gonzalez A, Granell J, Moragas R, Solans X, Font-Bardia M. J Chem Soc Dalton Trans 1998;1781.
[27] Gup R, Kirkan M. Spectrochim Acta Part A 2005;62:1188.
[28] Sreekanth A, Kala UL, Nayar CR, Kurup MRP. Polyhedron 2004;23:41.
[29] Gup R, Giziroglu E, Kırkan B. Dyes Pigments 2007;73:40.
[30] Maiti D, Paul H, Chanda N, Chakraborty S, Mondal B, Puranik VG, et al. Polyhedron 2004;23:831.
[31] Albert J, Gonzalez A, Granell J, Moragas R, Puerta C, Valerga P. Organometallics 1997;16:3775.
[32] Garg BS, Sharma RK, Kundra E. Transition Met Chem 2005;30:552.
[33] Omar MM, Mohamed GG. Spectrochim Acta Part A 2005;61:929.
[34] El-Dissouky A, Al-Fulij O, Kandil SS. J Coord Chem 2004;57:605.
[35] Charette J, Neirynck G, Teyssie P. J Phys Chem 1961;65:735.
[36] Sultan R, Gadamsetti K, Swavey S. Inorg Chim Acta 2006;359:1233.
[37] Leznoff CC, Lever ABP. Phthalocyanines properties and applications, vol. 4. VCH Publishers; 1996.
[38] Cao XZ, Zhang WH, Du YG. Inorganic chemistry. Beijing: Higher Education Press; 1983.
[39] Yilmaz I, Cukurovali A. Transition Met Chem 2003;28:399.
[40] Coats AW, Redfern JP. Nature 1964;201:68.
[41] Vinodkumar CR, Muraleedharan Nair MK, Radhakrishnan PK. J Therm Anal Calorim 2000;61:143.
[42] Kandil SS, El-Hefnawy GB, Baker EA. Thermochim Acta 2004;414:105.